systems (nonlinear systems with memory) driven by harmonic and Gaussian inputs," *Proc. IEEE*, vol. 59, pp. 1688–1707, Dec. 1971.
[6] "Communication receiver interference modeling," in *Proc. 1972 IEEE Int. Conf. Communications*, June 19–21, 1972, Session 30.
[7] A. L. Berman and C. E. Mahle, "Nonlinear phase shift in traveling-wave tubes as applied to multiple access communications satellites," *IEEE Trans. Commun. Technol.*, vol. COM-18, pp. 37–48, Feb. 1970.
[8] O. Shimbo, "Effects of intermodulation, AM–PM conversion, and additive noise in multicarrier TWT systems," *Proc. IEEE (Special Issue on Satellite Communications)*, vol. 59, pp. 230–238, Feb. 1971.
[9] H. C. Poon, "Modeling of bipolar transistor using integral charge-control model with application to third-order distortion studies," *IEEE Trans. Electron Devices*, vol. ED-19, pp. 719–731, June 1972.
[10] I. Tanaka *et al.*, "Nonlinear distortion and second harmonics in traveling-wave tubes," *Electron. Commun. Japan*, vol. 55B, pp. 62–68, 1972.
[11] *Transmission Systems for Communications*, 4th ed., Bell Labs., 1970, ch. 10.
[12] E. F. Cook, private communication, 1973.
[13] "Thin film on sapphire amplifier improves performance, is smaller," *Microwaves*, Aug. 1970.
[14] F. C. McVay, "Don't guess the spurious level," *Electron. Des.*, vol. 3, pp. 70–73, Feb. 1, 1967.
[15] F. F. Fulton, "Two-tone nonlinearity testing, the intercept point, P_I," Panel Session on "Nonlinearities in microwave devices and systems," in *Digest 1973 IEEE G-MTT Int. Microwave Symp.* (Boulder, Colo.), June 4–6, 1973, p. 112.
[16] ——, private communication, 1973.
[17] R. C. Heidt, "Three-tone nonlinearity testing—The intermodulation coefficient, M," Panel Session on "Nonlinearities in microwave devices and systems," in *Digest 1973 IEEE G-MTT Int. Microwave Symp.* (Boulder, Colo.), June 4–6, 1973, p. 113.
[18] H. Seidel, "A microwave feed-forward experiment," *Bell Syst. Tech. J.*, vol. 50, pp. 2879–2916, fig. 17, Nov. 1971.
[19] J. C. Gillespie, "Noise loading of FM systems—The noise-power-ratio, NPR, and customer requirements," Panel Session on "Nonlinearities in microwave devices and systems," in *Digest 1973 IEEE G-MTT Int. Microwave Symp.* (Boulder, Colo.), June 4–6, 1973, p. 113.
[20] R. B. Swerdlow, "Pseudo-random noise loading for system evaluation," Panel Session on "Microwave noise measurement and system effects," in *Digest 1973 IEEE G-MTT Int. Microwave Symp.* (Boulder, Colo.), June 4–6, 1973, p. 227.
[21] Y. L. Kuo, "Noise loading analysis of memoryless nonlinearity characterized by a Taylor series of finite order," to be published.
[22] R. C. Heidt, private communication, 1973.
[23] R. B. Swerdlow, private communication, 1973.

Broad-Band Microwave Measurements on GaAs «Traveling-Wave» Transistors

RAYMOND H. DEAN, MEMBER, IEEE, ARTHUR B. DREEBEN, JOHN J. HUGHES, MEMBER, IEEE, RALPH J. MATARESE, AND LOUIS S. NAPOLI, MEMBER, IEEE

***Abstract*—Instantaneous gain, noise figure, reverse attenuation, and gain and phase control measurements in the frequency range 8–18 GHz have been performed on GaAs traveling-wave transistors. The broad-band high-gain nature of the device together with the requirement for several bias connections precluded the use of standard test fixtures, and resulted in a package design exhibiting less than 1-dB insertion loss over the band together with 75- to 90-dB internal isolation. Untuned X-band gain, noise figure, and reverse attenuation were 12 dB, 18 dB, and 32 dB, respectively, and the gain and phase could be electronically varied over a 35-dB and 360° range. When RF tuning was employed, the gain, on the average, improved by 10 dB.**

I. Introduction

In 1967 Robson *et al.* [1] published a concise description of a two-port amplifier that made special use of the growing space-charge waves which travel unidirectionally from cathode to anode in a slab of n-type GaAs biased above the transferred-electron threshold. The high internal gain and built-in isolation made the device potentially attractive, but the use of closely compensated bulk material forced the authors to use pulsed biasing and placed constraints on the geometry which limited the net gain to several decibels and made the gain fall off rapidly above a few gigahertz.

Manuscript received May 14, 1973; revised July 12, 1973. This work was supported by the Air Force Avionics Laboratory, Wright-Patterson AFB, Ohio, under Contract F33615-72-C1616.

The authors are with the RCA Corporation, Princeton, N. J.

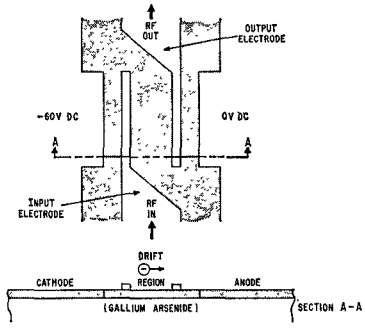

Fig. 1. Schematic of initial RCA traveling-wave transistor.

In 1970 Dean *et al.* [2] fabricated a similar device using 2-μm-thick epitaxially grown n-on-insulating GaAs. Because of the use of purer epitaxial material, dc biasing could be employed, and a more favorable geometry was obtained (see Fig. 1). The geometry employed in the epitaxial device resulted in significant unidirectional net gain in X band (8–12 GHz). The RF coupling electrodes on this device acted as Schottky-barrier electrodes, and in subsequent work, described in a 1972 paper by Dean and Matarese [3], it was shown that the input portion of the device behaved very much like a field-effect transistor. An EM wave propagating on the input line, shown in Fig. 1, produces a voltage. This voltage drives a conduction current, which establishes a fluc-

tuating charge, and the main-bias field carries this fluctuating charge away from the input FET section of the device as a traveling space-charge wave [4]. Whatever growth is present in the traveling space-charge wave amplifies the signal as the wave moves toward the output. At the output electrode the space-charge wave dumps its charge into the output circuit, thereby converting the signal into an EM wave again.

The relatively large distance between input and output electrodes (several space-charge wavelengths) provides isolation as well as space-charge-wave gain, thus allowing a very high gain–bandwidth product. The maximum broad-band stable gain is limited by two forms of output-to-input feedback. There is an internal feedback mechanism which is essentially the same as the feedback mechanism that causes supercritical Gunn diodes to oscillate. There is also an external or circuit feedback mechanism associated with coupling between the output and input transmission lines. The internal feedback mechanism limits the traveling-wave gain to less than about 30 dB [5]. It is fundamental to the traveling-wave part of the device and is not easily modified. The external feedback can be made almost arbitrarily small by proper device design [3] and good packaging.

II. Fabrication and Packaging

A. Device Construction

Epitaxial growth and subsequent processing is outlined below and refers to the device cross section in Fig. 2.

The first step in the fabrication of the GaAs traveling-wave transistor is the deposition of multilayer homoepitaxial GaAs, using a vapor-phase system [6]. Starting with a polished chromium-doped semi-insulating GaAs substrate oriented 3° off (100), 1 μm of n-type GaAs with a density of 5×10^{15} cm^{-3} is grown. Then, on top of this, a highly doped n^+ capping layer about 0.5 μm thick is grown.

Separate metal depositions form the ohmic contact electrodes and Schottky-barrier electrodes. The GaAs is etched preceeding the Schottky-barrier metallization. This exposes the channel and space-charge regions (n layer), while keeping the cathode (n^+) contact intact. Mesa etches remove epitaxial material outside the active regions, thereby reducing external parasitics.

A plan view of the final pattern is shown in Fig. 3. By comparing Figs. 2 and 3 with Fig. 1, and keeping in mind the presence of the n^+ layer in the present devices, one can see that even though the basic design is the same as that reported in [3], there are several differences in detail.

1) The new devices have the semiconducting material removed outside the region covered by the input electrode. A result is that there is no path around the end of the input electrode for extra (uncontrolled) traveling-wave current. This increases the range over which we can do voltage-controlled phase shifting at constant gain.

2) The semiconducting material between the output electrode and the large grounded screen at the anode end has been completely removed. A result is that there is no positive (or negative) conductance between the output electrode and the adjacent ground plane. This improves our ability to tune the output for maximum gain.

3) The input electrode is self-aligned and therefore is positioned very close to the cathode. In addition, n^+ material is used under the alloy contact to reduce contact resistance, thus reducing the parasitic source resistance to a relatively small value.

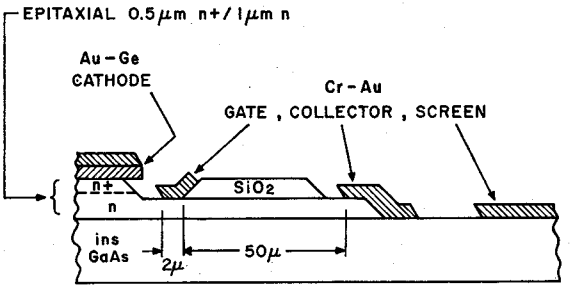

Fig. 2. Schematic cross section of new device structure.

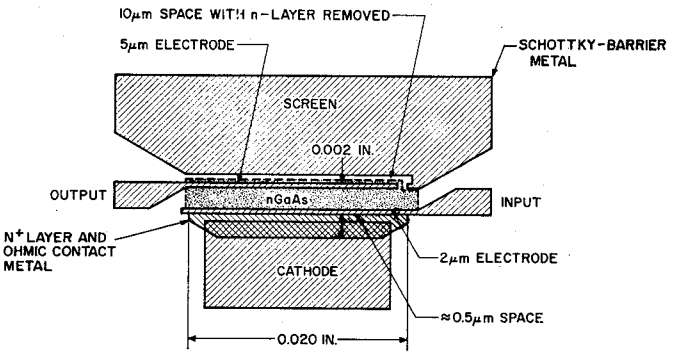

Fig. 3. Plan view of new device structure.

B. Packaging

1) OSSM 50-Ω Package: Fig. 4 shows a top view of a new microwave package with a traveling-wave transistor mounted in the center. The package is made by sandwiching a 0.060-in-thick copper plate between a pair of modified omnispectra subminiature (OSSM) connectors. Two bias leads are provided by fitting insulator-covered wires up through holes in the copper plate. Capacitors on top tie these bias leads to microwave ground. After device mounting, a grounded metal cap is bolted over the top to help reduce feedthrough between the OSSM connectors.

2) Header Package: To provide room for close-connected microwave tuning elements and a larger number of internal bias connections, a relatively sophisticated microwave package shown in Fig. 5 was developed. The transistor chip and all of its associated bias and microwave circuitry are mounted on a modified 10-pin integrated-circuit header, which is then positioned in a simple copper block for spring-contact with a pair of standard omnispectra miniature (OSM) connectors. All bias connections are made to the pins on the integrated circuit header, and flip-chip capacitors are used as dc blocks. Some microwave tuning elements can be included, since there is about one-quarter wavelength between the device chip in the center of the header and the ends of the OSM connectors at the edges of the header.

A metal plate (not shown in Fig. 5) inserted in the hole in the top of the package screens the input circuitry from the output circuitry. When this metal plate is in position, and a straight-through section is substituted for the device, the overall package transmission loss is less than about 1 dB from 6 to 18 GHz. With an open-circuit substitute for the device, the stray input-circuit to output-circuit transmission ranges from −90 dB at 8 GHz to about −75 dB at 18 GHz. Thus, in addition to being convenient and flexible, this package exhibits excellent microwave properties.

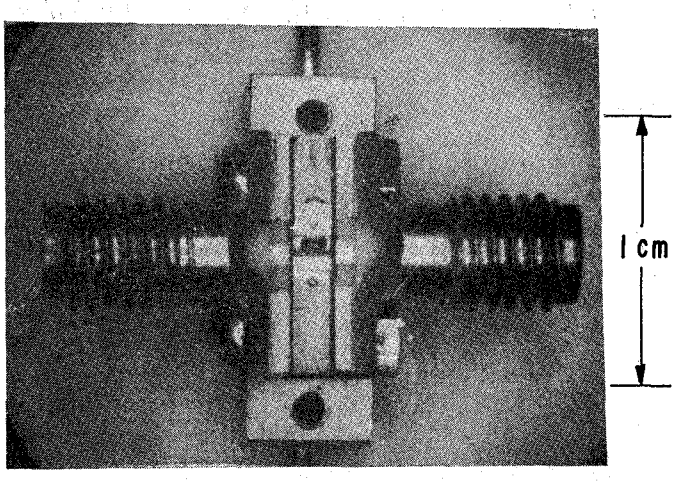

Fig. 4. OSSM 50-Ω microwave package with grounding cap removed.

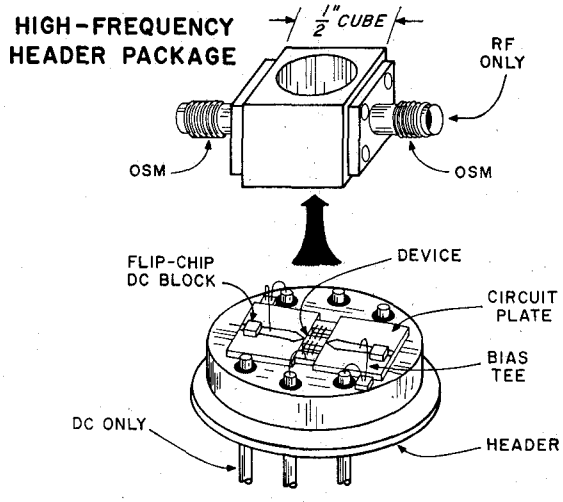

Fig. 5. Header package for multiple-bias *X*- and *KU*-band devices.

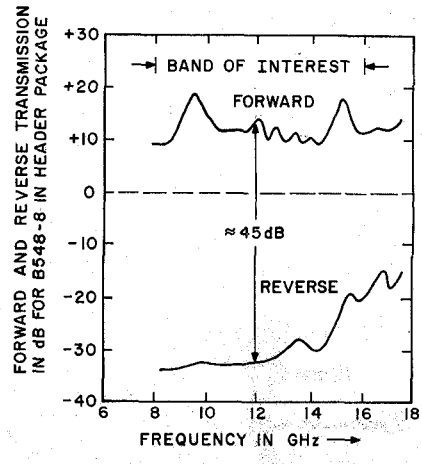

Fig. 6. Instantaneous forward and reverse net gain for new device mounted in header package. Displayed results include effects of all (built-in) bias T's and blocking capacitors.

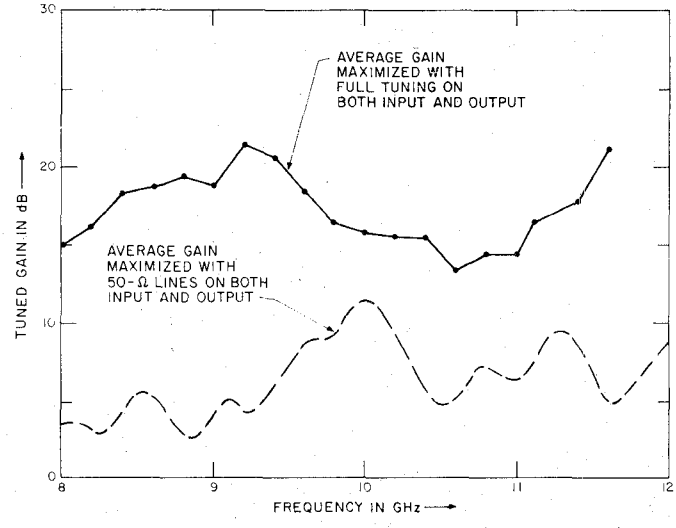

Fig. 7. Effect of external tuning on net gain for sample B-548-15.

III. Microwave Performance

A. Gain, Bandwidth, and Isolation

The curves in Fig. 6 show instantaneous net gain versus frequency for sample B-548-8. This device was mounted in the header package, and the displayed results represent instantaneous net gain for the device and the package, looking into 50-Ω input and output. The upper curve shows the transmission gain in the forward direction, and the lower curve shows the reverse gain. All the biases are on and fixed during these measurements. One can see that the forward-to-reverse gain ratio of the operating packaged device is about 45 dB at 12 GHz.

To see how tuning might be employed to improve gain and bandwidth, another sample from this same wafer (B-548-15), was mounted in the OSSM package, with input and output tuning provided by *X*-band waveguide slide-screw tuners. With the slide-screw tuners withdrawn and ineffective 5–10-dB net gain was exhibited through the 8–12-GHz frequency range (dashed line in Fig. 7). Without changing the bias conditions, the slide-screw tuners were inserted and adjusted to maximize the oscillation-free gain at 200-MHz intervals. The resulting curve is shown as the solid line in Fig. 7. Because the tuning was readjusted at each frequency, this is not, as before, an instantaneous gain curve, but it does show that the gain can be increased significantly (approximately 10 dB) by proper matching. Input and output impedance measurements show that while the device input impedance was fairly well matched to a 50-Ω coaxial line, the output impedance was much higher than 50 Ω. Thus it appears that the primary effect of the tuning was to provide a better match to the relatively high impedance of the traveling-space-charge waves at the output. To realize the full benefit of this tuning feature, one must provide a circuit which can match the device's output impedance over a relatively broad bandwidth.

B. Noise Figure

Our best noise figure to date has been obtained from sample B-548-6. Although this sample was taken from the same wafer that produced our best gain and bandwidth results, we were able to obtain only about 8-dB average maximum stable gain in *X* band from this unit. The device was mounted in the OSSM package, with external bias T's leading to untuned *X*-band waveguide. Fig. 8 shows instantaneous noise figure for the device and package along with the concomitant gain for one particular set of bias conditions. This set of conditions was selected for the best noise figure over a broad bandwidth. The lowest noise figure obtained in this measurement was

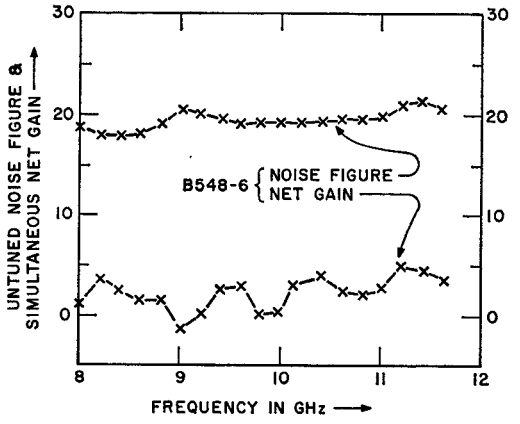

Fig. 8. Instantaneous noise figure, with 50-Ω input and output transmission line.

17.7 dB and the noise was nearly flat over a very broad frequency range. (No tuning was used this time.) With other bias conditions, we obtained a slightly lower minimum noise figure and higher gain at the minimum noise condition, but the average X-band noise figure was higher. With biases for near-maximum average X-band gain, the X-band noise figures typically rose to 21–25 dB. Input tuning did not seem to help much, suggesting that a significant amount of input dissipation was present.

C. Signal-Processing Capabilities

To evaluate the signal-processing capabilities of our more recent devices, we took the same device as that used to obtain the relatively high tuned gain shown in Fig. 7, and set up the tuning for maximum gain at 9 GHz. The cathode-to-output bias voltage was set at 47 V and held there to maintain a nearly constant phase. Then we modulated the input electrode bias to reduce the gain and obtained the output-versus-input characteristics shown in Fig. 9. The net gain was modulated over about 35 dB from -21 to $+14$ dB by varying the gate voltage from -6 to $+1$ V. As the gain changes, the saturation power varies also. For current levels below about 3 mA, the theoretically predicted [3] $P_{sat} \sim I^2$ dependence was followed. For automatic gain control, one would ideally like to have no saturation power variation with the gain modulation. Although we cannot attain this ideal condition, the 10-dB saturation power variation for 35-dB gain variation is quite good. The results also show that the attenuation introduced (in decibels) is directly proportional to the square of the applied negative gate bias, over most of the modulation range above. The relative simplicity of the functional dependence is important for practical applications.

Using the same device, we also looked at the 9.0-GHz phase-modulation capability. For this experiment we adjusted the voltage between cathode and input electrode to hold the net gain constant at $+7$ dB ± 0.5 dB as we varied the voltage between the input gate and output contact to vary the input-to-output phase shift. The mechanical tuners were fixed throughout. The results are shown in Fig. 10. One can see that we were able to obtain almost 360° phase shift with this constant gain. (Other experiments have shown that the phase shift produced by a given voltage change is proportional to frequency, so the corresponding 18-GHz phase shift is roughly twice this, or almost 720°.) Fig. 10 shows that the phase varies almost linearly with voltage over most of the range. The required associated modulation of the voltage between the cathode and the input gate was relatively small and for most of the 360° it could have been obtained "automatically" with a relatively simple compensating network in the dc biasing circuit. Thus the phase-shifting properties of the device are smoothly varying and large in extent.

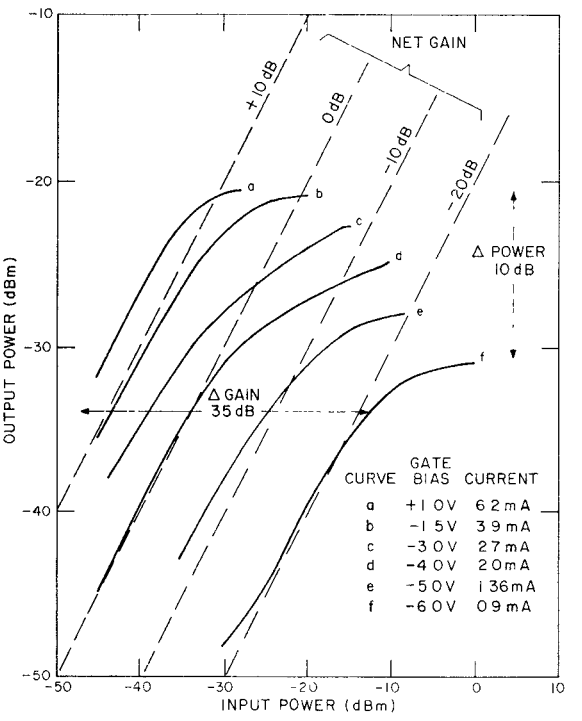

Fig. 9. Voltage-controlled gain-modulation characteristics for sample B-548-15 at 9.0 GHz. The voltage between cathode and output was held constant for nearly constant phase.

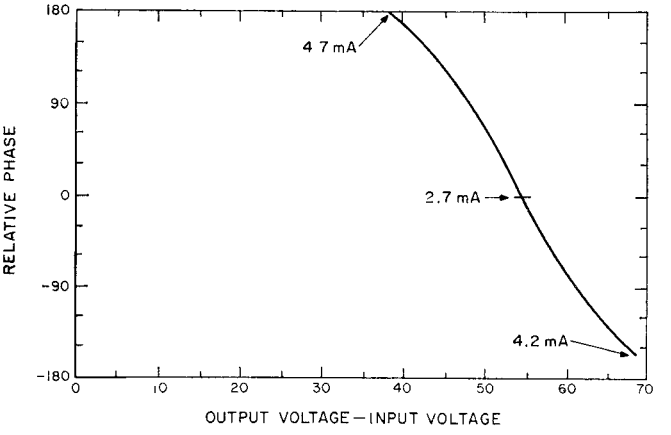

Fig. 10. Voltage-controlled phase-modulation characteristic for sample B-548-15 at 9.0 GHz. The voltage between cathode and input electrode was adjusted through a small range to hold the net gain constant at 7.0 ± 0.5 dB.

IV. Conclusions

The traveling-wave transistor, a thin-film GaAs device, has been tested for broad-band microwave performance. The low insertion loss and parasitic feedback of the microwave

test packages used allowed us to measure device properties over the band 8–18 GHz. The broad-band gain was on the average, 12 dB and reverse attenuation was about 32 dB. Tuning improved the gain by as much as 10 dB, primarily by improving the match between the output circuit and the traveling-wave region. Measured noise figure was about 18 dB, and it was limited by the inability to tune the input and by constraints which the traveling-wave region impose on the input FET section.

The gain of the device has been electronically varied over approximately 35 dB by varying the input gate voltage. The gain in dB was nearly proportional to the square of the gate voltage, and it was limited at the upper end by stability and at the lower end by capacitive feedthrough. The phase shift was nearly proportional to the input-to-output voltage change, and it was limited by the extent of the negative-mobility portion of the velocity-field curve. Future work will concentrate on techniques for improving noise figure and increasing output power capability.

ACKNOWLEDGMENT

The authors wish to thank A. R. Triano, Jr., for growing the epitaxial material. R. E. DeBrecht designed the OSSM package and helped to evaluate device performance. N. S. Klein and R. E. Chamberlain participated in the development of the microwave packages. H. Sobol provided helpful guidance.

REFERENCES

[1] P. N. Robson, G. S. Kino, and B. Fay, "Two-port microwave amplification in long samples of gallium arsenide," *IEEE Trans. Electron Devices* (Corresp.), vol. ED-14, pp. 612–615, Sept. 1967.
[2] R. H. Dean, A. B. Dreeben, J. F. Kaminski, and A. Triano, "Traveling-wave amplifier using thin epitaxial GaAs layer," *Electron. Lett.*, vol. 6, p. 777, 1970.
[3] R. H. Dean and R. J. Matarese, "The GaAs traveling-wave amplifier as a new kind of microwave transistor," *Proc. IEEE*, vol. 60, pp. 1486–1502, Dec. 1972.
[4] R. H. Dean and B. B. Robinson, "Space-charge waves in partially depleted negative-mobility media," to be published in *IEEE Trans. Electron Devices*, vol. ED-21, Jan. 1974.
[5] R. H. Dean, "Reflection amplification in thin layers of n-GaAs," *IEEE Trans. Electron Devices*, vol. ED-19, pp. 1148–1156, Nov. 1972.
[6] J. J. Tietjen and L. R. Weisberg, *Appl. Phys. Lett.*, vol. 7, p. 1, 1965.

RF Amplifier Design with Large-Signal S-Parameters

WILLIAM H. LEIGHTON, MEMBER, IEEE, ROGER J. CHAFFIN, MEMBER, IEEE, AND JOHN G. WEBB, MEMBER, IEEE

Abstract—**High-power UHF transistors have been characterized through the use of large-signal *S*-parameters. These *S*-parameters have been used successfully to design UHF power amplifiers. Waveform measurements show that due to the *Q* of the package parasitics, most class C operated UHF power transistors have nearly sinusoidal waveforms at their package terminals. Experimental evidence presented shows that the large-signal *S*-parameters are relatively independent of power once the device is turned on. These two observations make it possible to extend modified small-signal *S*-parameter design techniques to large-signal power amplifiers.**

I. INTRODUCTION

THE USE OF *S*-parameters for characterization of small-signal linear microwave devices and circuits is well known [1]. *S*-parameters are a valuable tool in analytic design of linear microwave circuits [2] because of ease of measurement and the convenience of their use. Analytic design procedures, using *S*-parameters, are well developed for small-signal transistor amplifiers. Design of high-power microwave transistor amplifier circuits, however, has been a cut-and-try procedure because of the lack of similar analytic procedures for high-power devices. Characterization of high-power transistors by *S*-parameters would be useful also for predicting the stability of circuits, and would provide a more convenient means of testing and evaluating transistors for high-power applications.

In this paper it is shown that the linear concept of the *S*-parameter can also be used in large-signal transistor amplifier design. Results from the measurement of the large-signal *S*-parameters and the RF saturation voltage of a microwave power transistor are presented. This information is then used to analytically design a 1-GHz 18-W amplifier. The success of this amplifier design partially verifies the applicability of *S*-parameters and linear design techniques to design nonlinear class C amplifiers.

First, the variation of large-signal *S*-parameters with drive level and bias conditions is discussed. It is shown that over a wide range of power, with the exception of S_{21} the *S*-parameters are not a strong function of applied power, and that the voltage waveforms observed when measuring large-signal *S*-parameters are nearly sinusoidal. These results support the hypothesis that the transistor, although operating in class C, can be analyzed, at least approximately, by linear methods.

Next, a method is described for measuring the RF saturation voltage of microwave transistors. The measured *S*-parameters and saturation voltage are then used to design an amplifier, and the performance of the resulting amplifier is compared with that of a cut-and-try optimized amplifier.

Manuscript received May 16, 1973; revised August 8, 1973. This work was supported by the U. S. Atomic Energy Commission.

W. H. Leighton was with Sandia Laboratories, Albuquerque, N. Mex. 87115. He is now with TRW Semiconductors, Lawndale, Calif.

R. J. Chaffin and J. G. Webb are with Sandia Laboratories, Albuquerque, N. Mex. 87115.